

Supplementary Information for
Global Urban Demographic Change and Migration Patterns

Andrew Zimmer^{1,2*}, Cascade Tuholske^{1,2}, Andrea E. Gaughan³, Nina Brooks⁴

¹ Department of Earth Sciences, Montana State University, Bozeman, MT, USA

² GeoSpatial Core Facility, Montana State University, Bozeman, MT, USA

³ Department of Geographic and Environmental Sciences, University of Louisville, Louisville, KY, USA

⁴ School of Public Health, Boston University, Boston, MA, USA

*Corresponding Author: Andrew Zimmer

Email: andrew.zimmer1@montana.edu

This file includes:

Figures S1 to S6

Tables S1 to S3

SI References

Table S1. Demographic variables constructed for each urban settlement.

Variable	Calculation
Total Population (city-size)	Sum of all age-sex groups
Young population	Population of males and females aged 0-15
Working-age population	Sum of males and females aged 16-65
Old-age population	Sum of males and females aged over 66
Total dependency-ratio (UDR)	(young population + old population) / working-age population
Young dependency ratio	Young population / working-age population
Old dependency ratio	Old population / working age-population
Sex-ratio (USR)	(total male population / total female population) x 100
Young sex-ratio	(total young male population / total young female population) x 100
Working-age sex-ratio	(total working-age male pop. / total working-age female pop.) x 100

Old-age sex-ratio	(total old-age male population / total old-age female population) x 100
Number of births (2000-2020)	Sum age 0 for each year (subtracting a proportional allocation of migrants from previous year to account for 0-year old's that immigrated)
Number of deaths (2000-2020)	Sum of estimates of death rate in each city (calculated using ~10km gridded estimates of death rates between 2000-2019 from Niva et al., 2023)
Net-Migration (2000-2020)	Sum: Total population change - total number of births - total number of deaths

S2 - Detailed Statistics for Large Cities

Table S2: Largest 5 cities from each region with population balance statistics. ‘% Contribution from migration’ refers to the proportion of population change that was driven by migration. For example, if a city grew by 200 people, with a natural population increase of 100, this would be 50% driven by migration. Note: The region of ‘*L.A. & C.*’ refers to Latin America and the Caribbean, and ‘*N.A.*’ refers to Northern America.

City	Country	Continent	Total Population 2020	Population Change (2000-2020)	Total Births (2000-2020)	Total Deaths (2000-2020)	Natural Change (2000-2020)	Net Migration (2000-2020)
Cairo	Egypt	Africa	20,012,119	5,866,204	8,869,710	2,059,065	6,810,645	-944,441
Luanda	Angola	Africa	13,507,472	13,004,893	2,887,758	615,948	2,271,810	10,733,083
Lagos	Nigeria	Africa	13,071,476	6,083,526	5,472,951	2,431,454	3,041,497	3,042,029
Johannesburg	South Africa	Africa	7,586,291	3,339,392	2,118,596	1,395,360	723,236	2,616,156
Kinshasa	DRC	Africa	6,789,932	2,414,661	3,140,394	1,163,721	1,976,673	437,988
Guangzhou	China	Asia	45,576,039	18,532,914	6,171,050	3,307,667	2,863,384	15,669,530
Jakarta	Indonesia	Asia	37,585,649	15,639,017	9,747,580	4,016,604	5,730,975	9,908,042
Tokyo	Japan	Asia	34,593,863	4,596,394	5,491,952	5,397,371	94,581	4,501,813
Shanghai	China	Asia	29,171,289	14,311,570	2,869,434	2,585,274	284,160	14,027,410
Delhi	India	Asia	28,519,757	10,744,347	8,446,515	2,750,098	5,696,417	5,047,930
Moscow	Russia	Europe	14,757,453	3,248,183	1,957,188	3,995,909	-2,038,721	5,286,903
London	U.K.	Europe	10,265,773	2,285,733	2,441,523	1,344,460	1,097,062	1,188,671
Paris	France	Europe	10,154,091	1,300,946	2,548,002	1,194,969	1,353,033	-52,088
Madrid	Spain	Europe	5,613,360	1,757,201	973,835	629,480	344,355	1,412,846
Barcelona	Spain	Europe	4,357,232	1,108,099	773,623	693,504	80,120	1,027,979
Mexico City	Mexico	L.A & C.	19,967,471	2,828,206	5,829,163	2,133,697	3,695,466	-867,260
São Paulo	Brazil	L.A & C.	19,488,045	3,205,178	5,187,035	2,250,125	2,936,910	268,268
Buenos Aires	Argentina	L.A & C.	13,935,127	3,260,228	4,026,347	1,949,935	2,076,412	1,183,816
Bogota	Colombia	L.A & C.	10,123,963	4,837,689	2,079,843	741,888	1,337,955	3,499,735
Lima	Peru	L.A & C.	10,011,846	3,711,118	2,691,189	936,784	1,754,405	1,956,713
New York	United States	N.A.	16,299,690	804,766	4,004,426	2,653,205	1,351,221	-546,455
Los Angeles	United States	N.A.	14,896,967	1,820,470	3,776,333	1,864,336	1,911,996	-91,527
Chicago	United States	N.A.	6,875,359	6,394	1,832,660	1,139,786	692,874	-686,480
Toronto	Canada	N.A.	6,383,427	1,709,300	1,136,672	790,908	345,764	1,363,536
Dallas	United States	N.A.	5,801,312	1,914,498	1,524,338	627,423	896,915	1,017,583
Sydney	Australia	Oceania	3,350,903	1,525	883,938	444,599	439,339	-437,813
Melbourne	Australia	Oceania	3,088,784	3,805	750,488	400,040	350,447	-346,642
Perth	Australia	Oceania	1,113,497	1,843	270,551	134,304	136,246	-134,403
Auckland	New Zealand	Oceania	1,037,961	214,893	268,662	108,032	160,630	54,262
Brisbane	Australia	Oceania	871,440	839	212,659	102,741	109,918	-109,079

S3 - Young Sex Ratio

Young sex ratio (Fig. S1) is closely balanced at 100 in most all cities globally. Since this refers to children under the age of 15, we would expect these values to be more balanced than the working-age sex ratio, for example. We see some changes in young sex ratio across some cities, with a slight increase in the Middle East, North Africa (MENA) region, and a slight decrease in central Africa between 2000 and 2020.

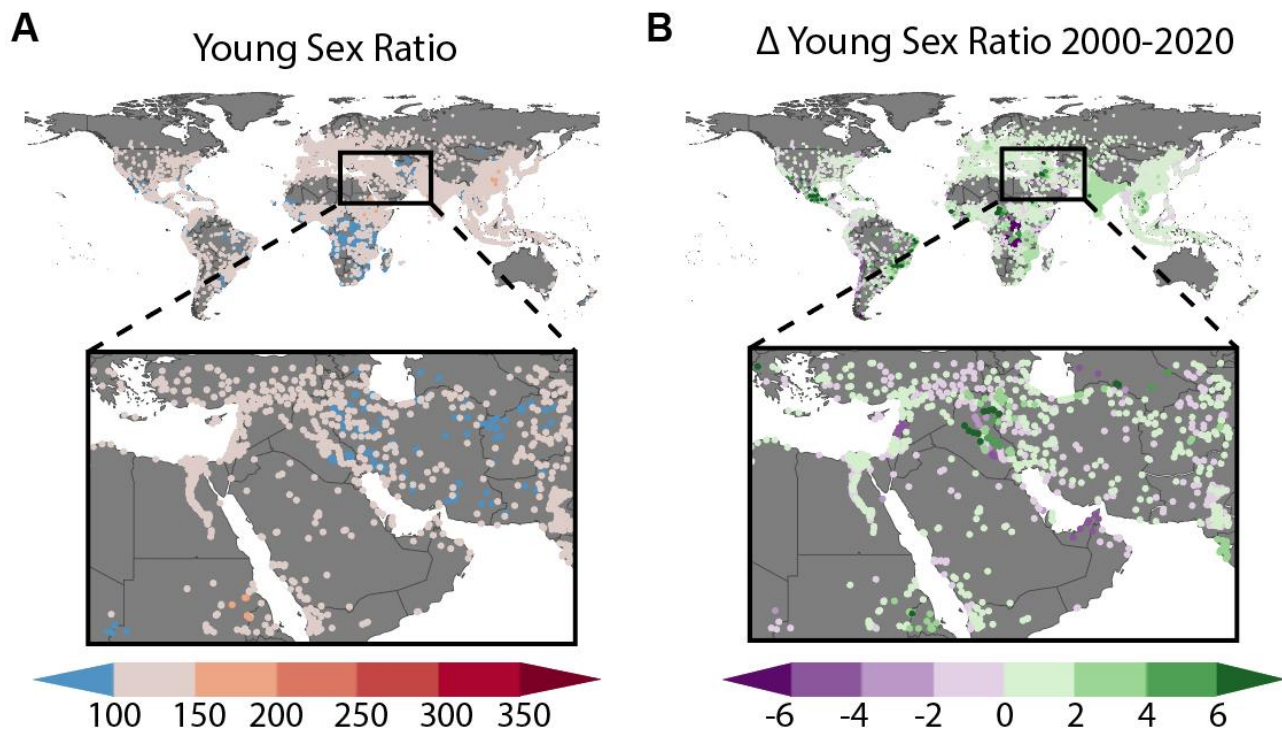


Fig. S1. Young-age sex ratio for each urban settlement in 2020 (A). Values range from 50-400 with a diverging color bar from 100. For reference, a value of 100 indicates the urban settlement has an equal population of young-age males, and young-age females. A value of 400 indicates 400 young males for every 100 young females. The change in the young sex ratio between 2000 and 2020 (B). An increase in the young sex ratio indicates a greater number of men, compared to women. Urban settlements colored green had an increase in young sex ratio, and those colored purple had a decrease. Note: For all maps, the highest value points are rendered last for emphasis.

S4 - Old Sex Ratio

Old sex ratio (Fig. S2) varies more regionally, with more females than males in most High-Income Countries (HICs) and some Low and Middle-Income Countries (LMICs). There are some cities in Eastern Africa and the MENA region with unbalanced male populations, even within the old-age category. Some cities in this region have many more males than females, such as Doha, Qatar where there are 174 males for every 100 females. In western Europe and North America, the old sex-ratio increased between 2000 and 2020 for 1,181 cities, and decreased for 250 cities, whereas in LMICs, the old-age sex ratio has decreased across most cities, with exceptions in central and southeast Africa, southeast Asia and some areas of South America.

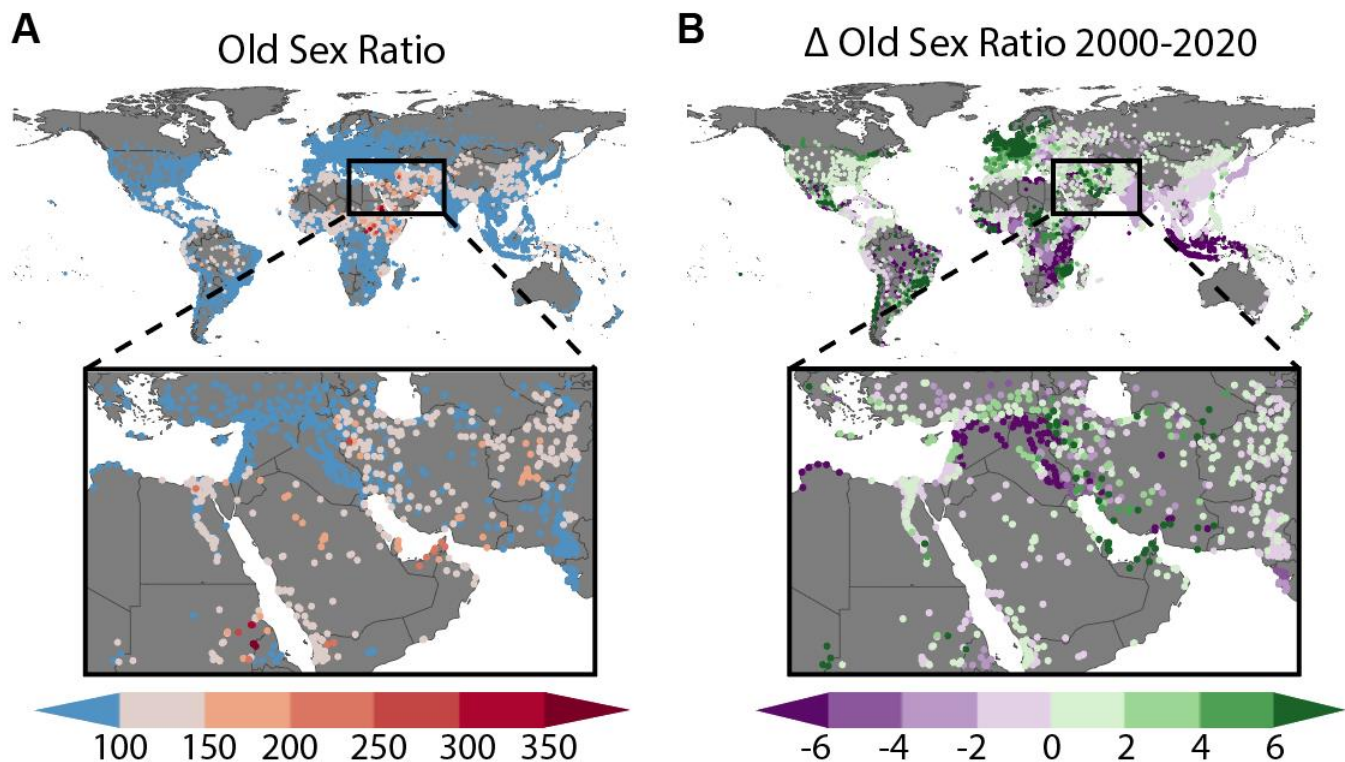


Fig. S2. Old-age sex ratio for each urban settlement in 2020 (A). Values range from 50-400 with a diverging color bar from 100. For reference, a value of 100 indicates the urban settlement has an equal population of old-age males, and old-age females. A value of 400 indicates 400 old males for every 100 young females. The change in the old sex ratio between 2000 and 2020 (B). An increase in the old sex ratio indicates a greater number of men, compared to women. Urban settlements colored green had an increase in old sex ratio, and those colored purple had a decrease. Note: For all maps, the highest value points are rendered last for emphasis.

S5 - Old Dependency Ratio

Old-dependency ratios (Fig. S3) are low across all city-sizes, and are generally increasing through time. Africa has the lowest old-dependency ratios across all city-sizes, due to very youthful populations. On the other hand, Asia has some of the largest – including two examples – outliers for old-dependency ratio, mostly driven by urban settlements in Japan, which are known to have aging populations. European cities have the highest average old-dependency ratio, which is also increasing through time.

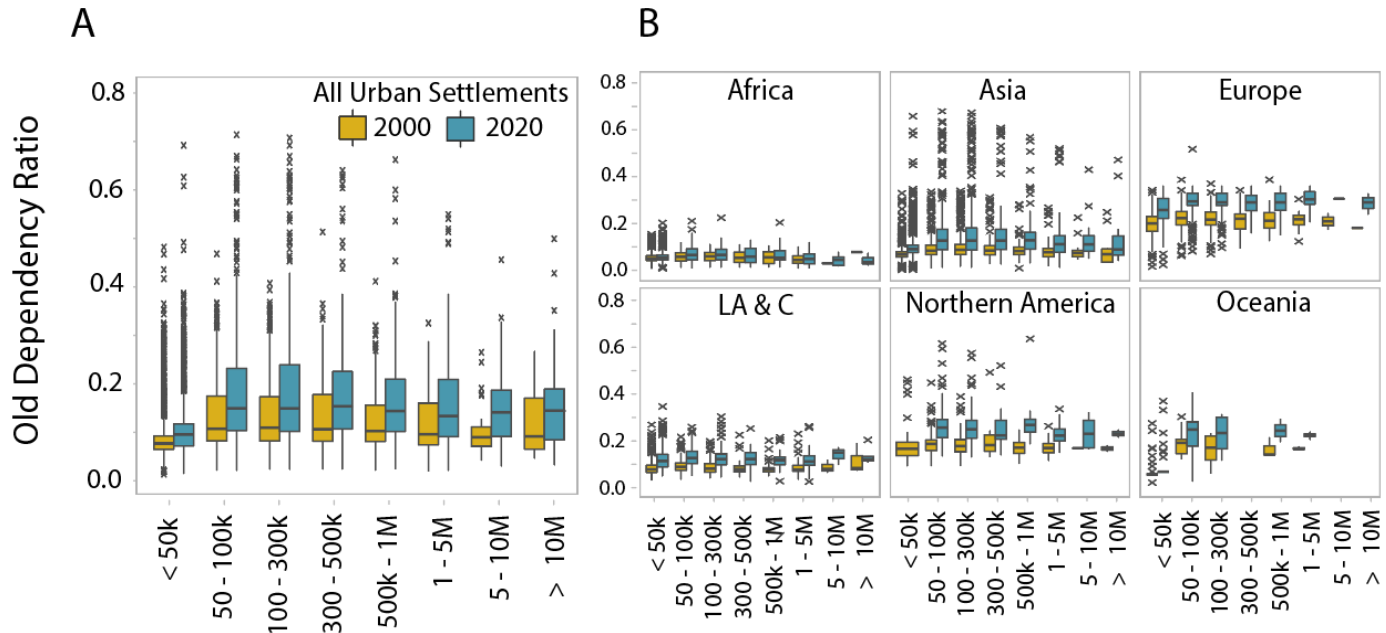


Figure S3. Distribution of old dependency ratio for all urban settlements (proportion of children compared to working-age adults) by city-size (A). Yellow boxplots show the distribution of old UDR in 2000 and blue boxplots show distributions in 2020. Distributions of old dependency ratio for all urban settlements, split by geographic region (B). The Y-axis is consistent across both A and B for comparison.

S6 - Total Dependency Ratio

Total-dependency ratios (Fig S4) reflect the young and old dependency ratios put together. They display a decreasing pattern across city-size, emphasizing our findings for young-dependency ratio and meaning that smaller cities typically have a larger share of dependents (children and older adults) than large cities. Regionally, these patterns reflect that of the young-dependency ratio with some of the highest average values in Africa, Asia and Latin America and the Caribbean. Total dependency ratios in Europe, Northern America and Oceania are relatively stable through time, but large decreases in total dependency ratio are found in Latin America and the Caribbean, as the population transitions from youthful, to being more balanced.

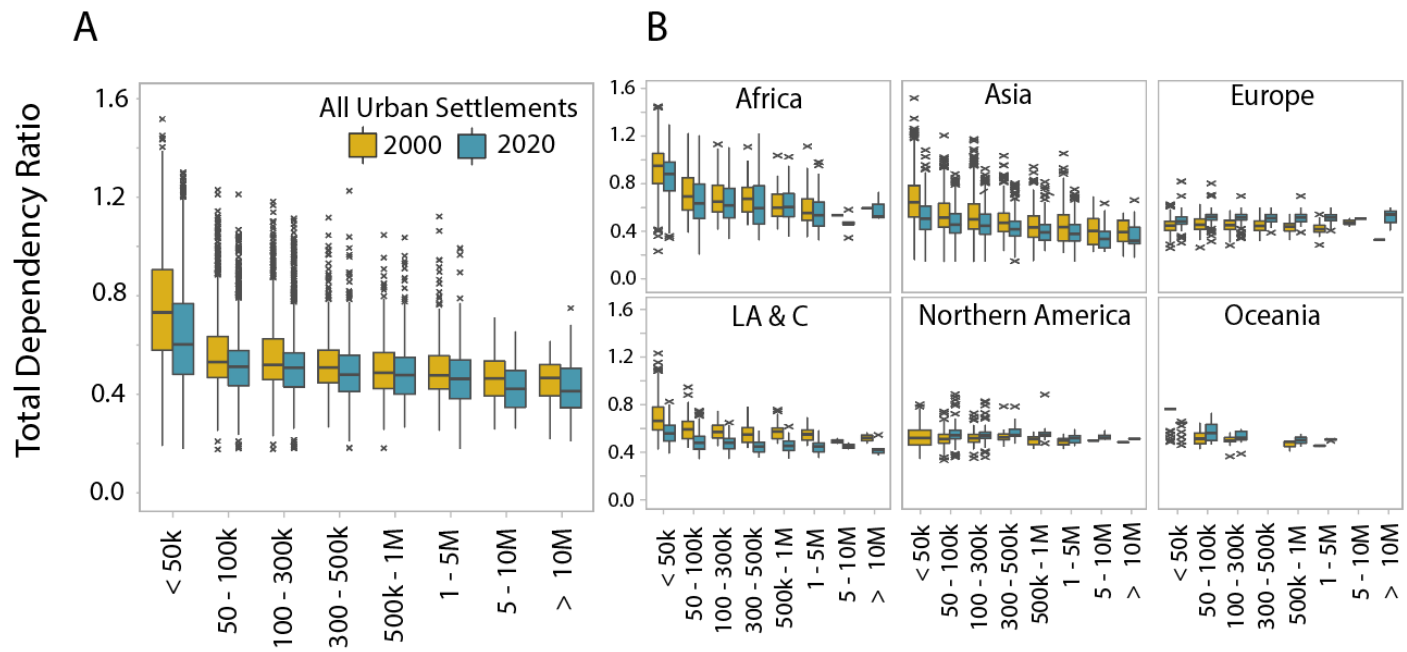


Figure S4. Distribution of total dependency ratio for all urban settlements (proportion of children compared to working-age adults) by city-size (A). Yellow boxplots show the distribution of UDR in 2000 and blue boxplots show distributions in 2020. Distributions of total dependency ratio for all urban settlements, split by geographic region (B). The Y-axis is consistent across both A and B for comparison.

S7 - Natural Growth v Migration Broken Down by Continent

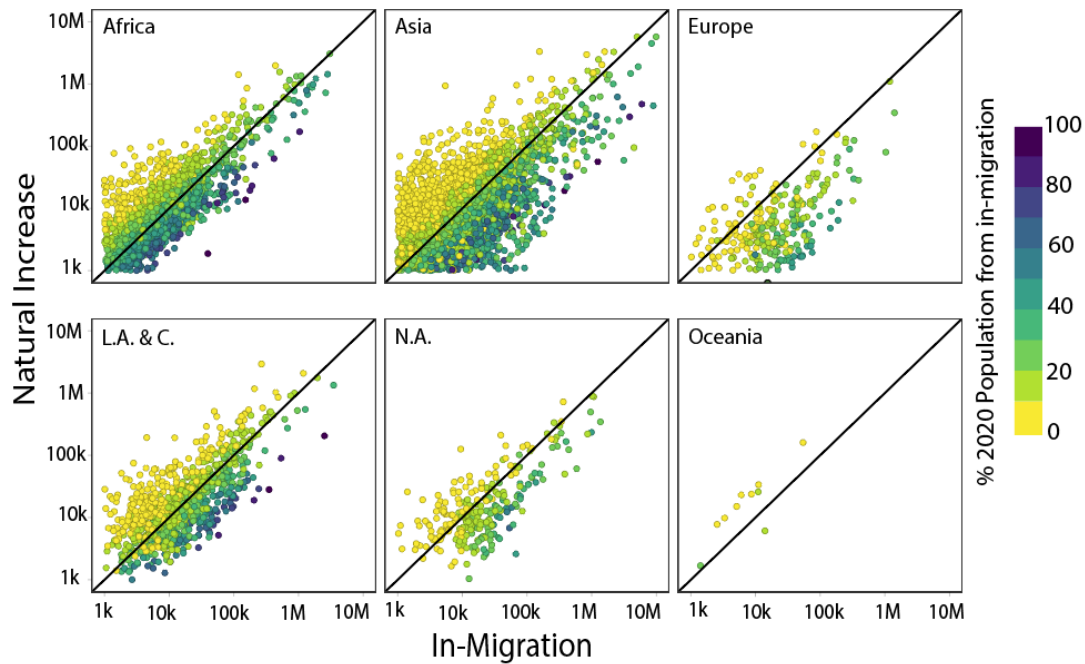


Figure S5. Distribution of cities with net-in migration and positive natural population growth. Colors represent the proportion of the 2020 population that in-migrated during the 2000-2020 period. Note: ‘L.A. & C’ refers to Latin America and the Caribbean and ‘N.A.’ refers to Northern America.

S8 - Gridded Death Rate v National Level (including 2019 v 2020)

Our estimates of natural population change, and thus, net-migration rely on using auxiliary datasets to estimate the number of deaths in each city through time. In order to do that, we use recently published gridded death rate data that is available at an annual timescale from 2000 to 2019.¹ This provides subnational variability in death rates that provides a more accurate picture of death rates and therefore migration than national level death rate statistics alone. In figure S6 we show a comparison of the number of deaths in each city in 2020 using national level data, and gridded data (the year 2019 is used for gridded data, since information on 2020 is not available using this gridded data product). We can see very close alignment in the number of deaths for most all cities, with a few exceptions in larger cities with high death rates. Typically, in these examples, national level death rates overestimate the actual number of deaths in the city concerned.

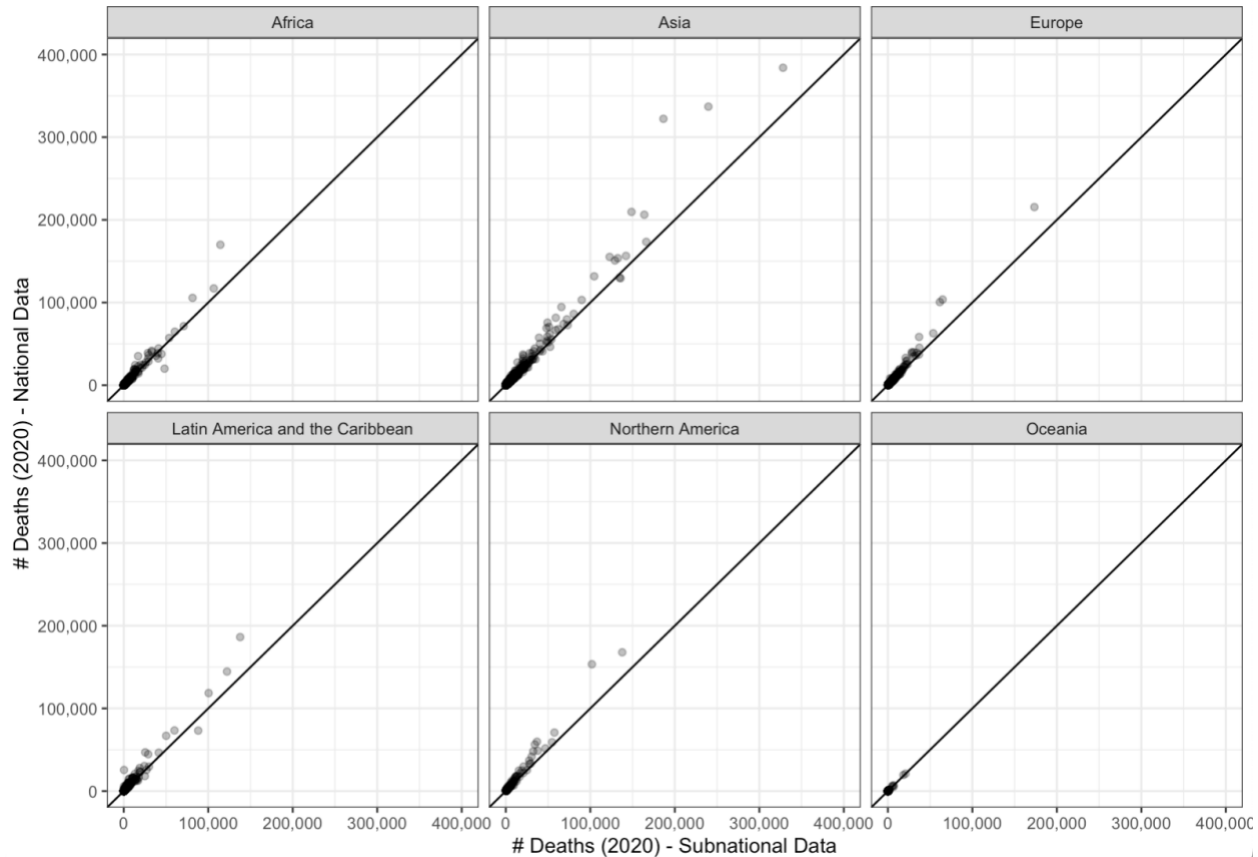


Figure S6: Estimate of the number of deaths in each city, using subnational, gridded data and national level data. The panels are split by continent and the diagonal line represents 1:1.

S9 - GHS-UCDB vs Changing Annual Boundaries from WorldPop

In our analysis we use the GHS-UCDB which represents a static urban boundary around the year of 2015, which does not account for expansion or contraction of the urban periphery. We use the GHS-UCDB dataset because it represents the only global dataset with place-based information about each city with a consistent methodology allowing us to track demographic structure through time^{2,3}. We can identify each city by name, making our data and results applicable to certain geographies and comparable with other analyses using the same urban spatial unit, including covariates such as extreme heat.⁴

Recognizing the static nature of the GHS-UCDB boundaries, we performed a sensitivity analysis. It is not possible to change the GHS-UCDB boundaries through time, and so we used the WorldPop age-sex data to derive urban boundaries through time, using the same population threshold as the GHS-UCDB ($>1,500$ people / km^2). The GHS-UCDB applies a secondary threshold using building density, where building density / km^2 must exceed 50%. WorldPop does not provide a building density layer alongside the age-sex data, and so we simply applied a $>1,500$ people / km^2 threshold and extracted urban boundaries through time. Using these new

urban boundaries, we checked and manually assigned them a city-location that matched the GHS-UCDB (available natively in the GHS-UCDB) so we could compare to our main sample. We then extracted the age-sex structure within these urban boundaries and calculated total population and dependency ratio for the cities for years 2000 and 2020, comparing below with our estimates using the GHS-UCDB boundaries.

When comparing the GHS-UCDB to the WorldPop boundaries that change through time, we find variability in total urban population measured, as to be expected. However, the difference in urban dependency ratio is much smaller, as the WorldPop age-sex structure is generated using the best available census data, some of which may not vary across urban/peri-urban areas within the same city, and therefore provide similar estimates of dependency ratio across similar spatial units.

Table S3: Estimates of total population and dependency ratio for a selection of cities using the GHS-UCDB boundaries and a similar urban boundary produced using WorldPop population data.

City	Country	Continent	Year	WorldPop Boundaries Total Population	GHS-UCDB Boundaries Total Population	WorldPop Boundaries Total Dependency Ratio	GHS-UCDB Boundaries Total Dependency Ratio
Chicago	U.S.A.	North America	2000	4,316,983	6,868,965	0.51	0.49
Chicago	U.S.A.	North America	2020	4,070,485	6,875,359	0.51	0.51
Chiclayo	Peru	South America	2000	609,090	369,728	0.49	0.60
Chiclayo	Peru	South America	2020	563,400	532,417	0.49	0.49
Christchurch	New Zealand	Oceania	2000	136,456	256,968	0.52	0.49
Christchurch	New Zealand	Oceania	2020	147,134	242,168	0.48	0.52
Crewe	U.K.	Europe	2000	50,755	67,796	0.60	0.54
Crewe	U.K.	Europe	2020	49,440	75,135	0.57	0.57
Hamburg	Germany	Europe	2000	339,820	1,476,571	0.54	0.44
Hamburg	Germany	Europe	2020	341,100	1,510,044	0.54	0.54
Hyderabad	India	Asia	2000	8,861,790	1,100,707	0.40	0.72
Hyderabad	India	Asia	2020	7,591,643	1,771,847	0.40	0.56
Jayapura	Indonesia	Asia	2000	203,751	35,661	0.52	0.61
Jayapura	Indonesia	Asia	2020	61,800	89,615	0.52	0.52
Kinshasa	D.R.C.	Africa	2000	7,055,627	4,375,271	0.61	0.70
Kinshasa	D.R.C.	Africa	2020	6,875,603	6,789,932	0.61	0.61
Kitwe	Zambia	Africa	2000	414,506	192,352	0.73	0.80
Kitwe	Zambia	Africa	2020	197,824	377,986	0.73	0.73
Mombasa	Kenya	Africa	2000	1,217,894	563,669	0.44	0.52
Mombasa	Kenya	Africa	2020	1,121,015	1,038,744	0.44	0.44
Nanning (南宁市)	China	Asia	2000	2,452,187	2,014,647	0.33	0.34
Nanning (南宁市)	China	Asia	2020	2,403,659	2,460,780	0.33	0.33
Paris	France	Europe	2000	9,145,231	8,853,145	0.62	0.47
Paris	France	Europe	2020	9,365,890	10,154,091	0.62	0.62
Pokhara	Nepal	Asia	2000	261,416	217,621	0.69	1.11
Pokhara	Nepal	Asia	2020	271,346	257,904	0.69	0.69
San Cristóbal de las Casas	Mexico	North America	2000	240,803	4,466	0.44	1.05

San Cristóbal de las Casas	Mexico	North America	2020	173,004	9,405	0.44	0.71
São Paolo	Brazil	South America	2000	19,609,647	16,282,866	0.39	0.46
São Paolo	Brazil	South America	2020	19,406,913	19,488,045	0.39	0.39
Salt Lake City	U.S.A.	North America	2000	650,702	795,102	0.53	0.53
Salt Lake City	U.S.A.	North America	2020	319,783	1,044,628	0.53	0.53
Sydney	Australia	Oceania	2000	2,782,150	3,349,377	0.49	0.45
Sydney	Australia	Oceania	2020	2,789,824	3,350,902	0.49	0.50
Victoria	Canada	North America	2000	115,077	191,574	0.53	0.46
Victoria	Canada	North America	2020	111,067	226,767	0.53	0.53

Supplementary Information References

1. Niva, V. *et al.* World's human migration patterns in 2000–2019 unveiled by high-resolution data. *Nat. Hum. Behav.* **7**, 2023–2037 (2023).
2. Florczyk, A. *et al.* GHS-UCDB R2019A - GHS Urban Centre Database 2015, multitemporal and multidimensional attributes. (2019).
3. Melchiorri, M. *et al.* The Multi-temporal and Multi-dimensional Global Urban Centre Database to Delineate and Analyse World Cities. *Sci. Data* **11**, 82 (2024).
4. Tuholske, C. *et al.* Global urban population exposure to extreme heat. *Proc. Natl. Acad. Sci.* **118**, e2024792118 (2021).